On Electrostatic Coupling in ICRH at the Plasma Edge

M.J. Alava and J.A. Heikkinen

Helsinki University of Technology, Department of Technical Physics,
SF-02150 Espoo, Finland

Abstract

The mechanisms leading to a concomitant coupling of electrostatic (ES) waves in ion cyclotron range fast wave heating experiments are studied. Mode conversion at the lower hybrid resonance and direct coupling to ES waves due to the misalignment of the antenna Faraday shields are considered as sources of intense ES waves in the edge plasma. Ion acceleration by wave trapping is suggested as a mechanism that restricts the amplitude of the parasitic modes and creates energetic ions.

1. Introduction

Experimentally, various edge effects are observed during ion cyclotron resonance heating. Increases in ion and electron temperatures indicate that some part of the coupled power is absorbed at the edge. Either due to an increased interaction with the plasma facing components or to some other process, the density profile at the edge often flattens, sometimes with a simultaneous increase in the edge density [8]. While the recent sheath-based theories [12] have been successful in explaining to a large degree the deleterious impurity production problems encountered, there is evidence for processes which may cause ion acceleration and sputtering of the plasma facing structures, not limited to the immediate vicinity of the antenna [24]. In making comparisons with experimental results, the dependences of harmful effects like sputtering or edge heating on the radiated total power, spectrum and antenna geometry play an important role. The coupling of electrostatic waves, which have recently been observed in a number of experiments [23,29], has a similar dependence on these parameters as the sheath-based models. Moreover, other not so localized effects, as e.g. the edge modification, appear to be more easily explained by the ES wave coupling.

In this paper, we study various possibilities for the parasitic coupling of the fast magnetosonic wave to electrostatic waves. These include mode conversion in front of the antenna at the lower hybrid (LH) resonance or by a steep density gradient, antenna geometry non-idealities which lead to a direct coupling of ES waves, and non-linear parametric interactions, in which the fast wave decays to lower frequency ES modes. The relative strengths of these processes are compared in section 2. Section 3 discusses the absorption of the coupled ES waves. In section 4 we outline the implications of ES coupling theory on experiments and discuss the limitations of what has until now been achieved on the theoretical side.

2. Mechanisms of Electrostatic Coupling

2.1 On waves in the edge plasma

To model the ES wave coupling at the edge plasma, three different wave modes have to be included. Their respective WKB-limit wavenumbers, correct to second order in ion Larmor radius, are given by $n^2_{\mathrm{FW}} = [(S-n_z^2)^2 - D^2]/(S-n_z^2)$, $n^2_{\mathrm{SW}} = -P(S-n_z^2)/S$ and $n^2_{\mathrm{IBW}} = S/\sigma$, where FW, SW and IBW denote the fast, slow and ion Bernstein waves and $n^2 = n_x^2 + n_y^2$; n_x, n_y and n_z are the radial, poloidal and toroidal refractive indices of a mode. S, D and P are the cold plasma dielectric tensor elements in the Stix' notation [27] and $\sigma = \sum_i 3/2\,(\omega_{p,i}^2/\Omega_i^2)\,(v_i^2/c^2)\,\omega^2\Omega_i^2/((\omega^2-4\Omega_i^2)(\omega^2-\Omega_i^2))$ gives the thermal correction to the dielectric tensor element ϵ_{xx}. Here $\omega_{p,i}$, Ω_i and v_i denote the plasma frequency, cyclotron frequency and thermal velocity of the i:th ion species. The fast wave experiences a resonance at the lower hybrid (LH) resonance where $S - n_z^2 = 0$, given a small enough n_z and density. At the same point, the slow wave undergoes a mode transformation to the IBW mode [25].

2.2 Linear mode conversion at the plasma edge

Recent experimental measurements of density profiles in the very front of Faraday screens (FS) have given strong evidence of electron densities of the order of 10^{15} - 10^{16} m^{-3} [28]. In such cases, the lower hybrid resonance may exist in the vicinity of the screen [2,4]. At the LH resonance, the fast wave couples to the electrostatic IBW mode. The strength of this process has recently been calculated in the limit of a long fast wave wavelength and for $n_z \ll 1$ [2]; the converted power flux in units of $c\epsilon_0$ is found to be

$$\Delta I = \pi \frac{|DE_y + n_y C_y|^2}{|S'|}, \tag{1}$$

where S' is the radial derivative of S at the LH resonance, E_y is the poloidal field of the incoming fast wave at the resonance and n_y is the poloidal refractive index of the mode. C_y denotes an integration constant, related to the radial derivative of the poloidal field with $dE_y/dx = in_y E_x + C_y$, which can be derived [2] from the 1-D wave equations in the limit of a short spatial extent of the conversion region.
This coupling process is closely related to the phenomenon of parasitic coupling by density gradient discovered by Skiff et al. [26]. Indeed, the linearization of the background plasma parameters around the resonance, which was used in deriving the expression in Eq. (1), can be circumvented by solving the equation for the radial field, corresponding to the IBW, in the limit of strongly inhomogeneous, exponential density profiles and with $n_z \simeq 0$, considering a pure ion Bernstein wave without the electron response. The resulting expression, given in refs [2,3] shows that one may consider both the processes to result from the rapid variation of the polarization ratio of the magnetosonic wave, $E_x/E_y \simeq (iD - n_y n_z)/(S - n_z^2 - n_y^2)$, where E_x is the radial field.
Usually, the wave equations have to be solved numerically. The techniques generally used are a finite element discretization, radiative boundary conditions at the end of the 1-D plasma slab to avoid global calculations, and simplified strap antenna models to excite the waves [5,2]. Fig. 1a compares the converted power flux calculated from Eq. (1) with the corresponding result from the numerical solution. A very good agreement is found in the limit of small coupling. Moreover, the figure demonstrates the dependence of the coupling processes on plasma density. The LH conversion, contrary to the density gradient excitation, is strongest when the density gradient is low. The both conversion mechanisms do not depend on temperature, a fact which can be deduced from Eq. (1), and applies also in the more general case of gradient coupling. Fig. 1b shows the coupled power fluxes as a function of n_y. For a non-zero n_y, ΔI can be fairly high. Again, a good agreement with the numerical result is found.

2.3 Coupling due to non-ideal antenna geometry

There exists two different processes in which a part of the heating power can directly end into the parasitic ES modes from the antenna. These are caused either by the fringing fields of the Faraday shield [11,14,18] or by the antenna field [13,20,6], due to the misalignment of the shields with respect to the background magnetic field. Both case have been analyzed by assuming a homogeneous plasma for the WKB-limit to hold for the coupled waves. In the absence of the fringing fields, the fraction of the total power coupled to the ES

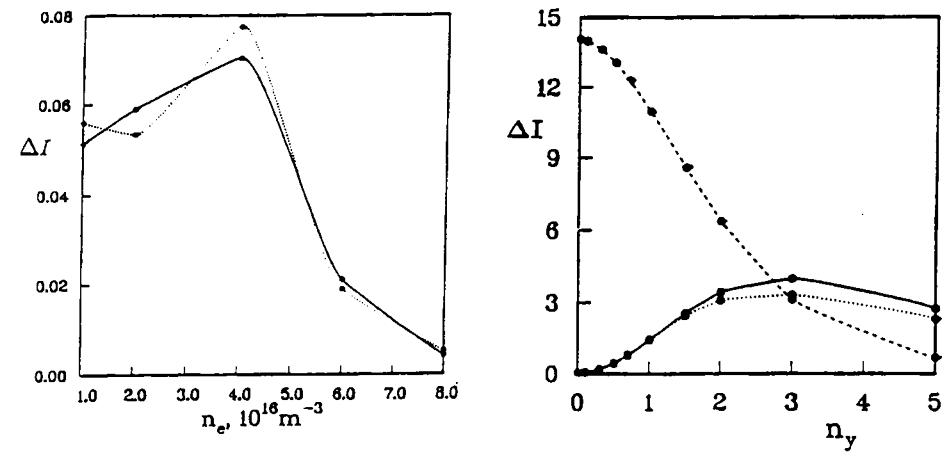

Figure 1: a) The analytically and numerically calculated converted energy fluxes as functions of screen density. The density profile is exponential, n_e at $x = 0.02$ m is roughly 2×10^{18} m^{-3} . The analytic estimate is given by the solid curve, and the numerical solution by the dotted one. A D–plasma, 5 % of the minority species H and ^{3}He. The magnetic field at the shield is 2.34 T, $\omega = 2.11 \times 10^8$ (1/s), $n_z = 0$, $n_y = 0$, $R = 4.15$ m at the shield and $T_0 =$ 30 eV, $T = 60$ eV at $x = 0.02$ m. b) The analytic (dotted) and numerical (solid) converted energy fluxes as functions of n_y for $n_z = 0$. $n_D = 10^{16}$ m^{-3} at the screen. The numerical coupled fast wave flux is shown also (dashed). Other parameters as in a).

modes is approximately $(P/n_{SW}\text{Re}[n_{FW}])\sin^2\beta$ for the slow wave coupling case ($S > 0$) and $[P(P - n_{SW}^2)/n_{IBW}^3\text{Re}[n_{FW}]]\sin^2\beta$ for the IBW coupling ($S < 0$). The strength of the coupling is in both cases proportional to $\sin^2\beta$, where β is the angle between the Faraday screen and the background magnetic field. The dependence of the coupling on plasma density and n_z depends on whether the slow or ion Bernstein wave propagates in front of the shield: in the first case the relative coupling reaches a maximum at small $n_z \leq 1$, while in the second case it is encountered at high values of n_z, which also presupposes a high enough density. If the coupling occurs through the IBW branch, the largest effect is achieved, as in the usual IBW coupling theory, when the first harmonic of an ion species is located just behind the antenna. In a numerical study [20] the converted power fractions 5 % and 1 – 2 % were calculated by integrating over the antenna spectrum for the JET monopole and dipole antennas, respectively. The model density profile included the LH resonance behind the antenna protecting limiters. The conversion was found to obey the dependence $\Delta I \simeq \sin^2\beta$, for large β. Given a decomposition of the antenna current to parallel and poloidal components, the linearity of the problem leads to the scaling $\sin^2\beta$ as long as there is no LH resonance and the relation $E_z = -\sin\beta E_a$ holds where E_a is the field at the screen without misalignment. This assumption has been questioned by a 2-D full wave calculation [21], in which the finite density between the screen blades was found to lead to a screening effect, reducing E_z for large densities. From the analytical predictions [18], the fringing fields have a tendence to enhance the ES wave coupling due to the misalignment of the screens. While the existence of the fringing field mechanism in experiments is by no means sure, there is however evidence for the coupling of the antenna field due to the misalignment. In the JET experiments with reversed toroidal field, producing a substantial misalignment [9], a change in the coupling resistance and impurity production was detected.

2.4 Parametric decay at the edge

During intense ICRF heating by fast magnetosonic waves, decay of the fast wave to an ion Bernstein wave and an ion quasi-mode has been predicted theoretically [17] and observed in the scrape–off layer of tokamaks [31]. Also, parametric decay of the fast wave to resonant ion Bernstein waves or to an ion Bernstein wave and an electron quasimode [31] or the generation of half–harmonics [30] may occur in the scrape–off layer. It has been suggested that direct edge heating and the consequent enhancement of density and impurity production in some ICRF heating experiments could be partly due to these decay processes. However, no clear connection between the deleterious phenomena and the decay processes was found in recent JET experiments [7].

The inclusion of non–linear saturation mechanisms [19] in the fast wave decay indicates that the unstable modes may not reach much larger field levels than $E \simeq 100 - 500$ V/cm for typical scrape–off layer parameters (for a fast wave power flux less than about 3 MW/m^2). Consequently, the converted power fraction remains much below 1 %. Even at larger decay mode field levels ($E \simeq 1000$–2000 V/cm) near the wave breaking, the conversion amounts to only a few percent due to the finite interaction region and convective losses of the instability. It should be noted that the saturation of the instability is is an extremely complicated process, and, therefore, the results require further validation. We also note that the parametric processes depend strongly on the gradients of the background plasma parameters. In the very vicinity of the Faraday shields, the gradients are very steep which may restrain the growth of some instabilities while at the same time other decay processes, e.g. the half–harmonics decay [16], may be destabilized.

3. On electrostatic waves at the edge

We note that the IBWs generated through any of the processes mentioned in the previous chapter behave analogously to the corresponding modes at IBW heating experiments with a similar heating scheme. Thus the waves can be assumed to propagate rapidly radially into the plasma, and then to be absorbed at the cyclotron resonance layer if no competing effects exist as demonstrated by full–wave calculations [5,15]. In the case of IBW heating, the dependence of the wave propagation on the initial poloidal location or extent of the antenna has recently been invoked as an explanation for the failures of some experiments by Cardinali and Romanelli [10]. In principle, the mechanism could thus be expected to operate in cases in which the fast wave antenna is located away from the midplane, and to cause electron heating via Landau damping. The electron absorption of the ES power will otherwise remain fairly small, as the approximative polarization $E_z/E_x = -n_{IBW}n_z/P$ suggests. This is even more clear at low densities near the Faraday shield, in which case most of the ES coupling is expected to occur at low $n_z \simeq 0$ due to the LH resonance. We conclude from our analysis in section 2 that the parasitic coupling may at most amount to some 10 – 20 % of the total radiated antenna power. Thus the operating edge absorption mechanisms should be strong enough to cause noticeable effects at the edge.

Because of the low density and temperature at the edge, the IBW radial electric fields are fairly large. Using the estimate $\vec{S} = c\epsilon_0\sigma E_x^* dE_x/dx$ for the wave kinetic energy flux, we plot in Fig. 2a E_x as a function of ω/Ω for $\omega = 2\times 10^8$ s^{-1}. We assume a deuterium plasma, density 10^{18} m^{-3} and temperature 50 eV for an incoming energy flux 1 MW / m^2. The field level at which the energy density W of an IBW mode equals the plasma thermal energy density is shown for the same parameters, calculated from $W = \epsilon_0\omega\partial\epsilon/\partial\omega|E_x|^2$. We find that the wave energy is quite large as compared to the plasma kinetic one. Figure 2b shows, with the plasma parameters of Fig. 2a, the perpendicular energy distribution function of 1000

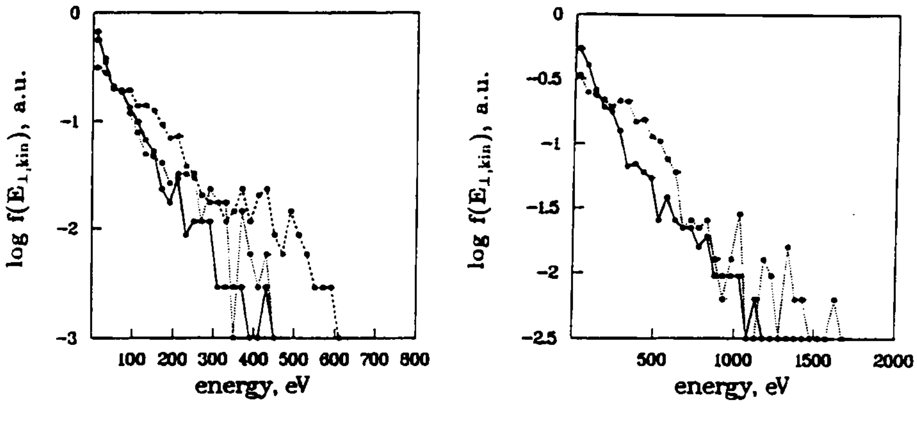

Figure 2: a) The electric fields at which the plasma kinetic energy equals the wave energy (solid curve) and for an IBW energy flux of 1 MW/m^{-2} (dotted) in the $n_z \simeq 0$ limit. b) ion energy distribution functions for E_0 = 500 (solid), 600 (dotted) and 700 (dashed) V/cm.

deuterons for an initially Maxwellian distribution after Δt = 200 $\times 1/\omega$ for various electric field values. It has been obtained by integrating the single particle equations of motion in a background magnetic field B_z = 2.34 T and an electrostatic field $E_x = E_0 \cos(\omega t - k_\perp x)$. Here we have chosen $k_\perp$ = 800 m^{-1}, corresponding to the approximate IBW perpendicular wave vector in the limit of small $n_z \ll 1$ and ω/Ω = 1.88. As the figure shows, significant heating is obtained if the electric field exceeds a threshold which roughly corresponds to the value where the wave is in thermal equilibrium with the background plasma, but is still well below the threshold for stochastic heating [1,22].

4. Discussion

We have given an overview of the different processes that may cause coupling of power to electrostatic waves at the plasma edge. The most powerful mechanisms can lead to an ES excitation of some 10 % of the coupled power. The remaining theoretical problems concern the boundary conditions assumed at the Faraday shield. There the total kinetic energy flux is usually set to zero at the shield–plasma interface, which requires further study. Also, the use of the finite Larmor radius expansion limits the scope of the results to cases in which the frequency is below the first harmonic of all the ion species.

Although the theoretical predictions agree with the experimental conclusion that monopole excitation of fast wave antennas leads to a strong interaction with the plasma edge, there still remains the question of the exact process by which the wave power is absorbed at the edge. The existence of high energy light ions in the edge plasma has been demonstrated by e.g. recent ASDEX results [32]. One possible production mechanism is ion trapping in the parasitically coupled electrostatic wave fields (see Fig. 2b). However, to quantitatively assess this idea the self-consistent plasma response should be evaluated, as well as other non-linear phenomena which might reduce the actual wave amplitudes.

Acknowledgements

The authors are grateful to Drs. M. Bureś and D.F. Düchs for discussions during this work. M.A. acknowledges financial support by the National Research Council for Technology, the Academy of Finland and by the Jenny and Antti Wihuri Foundation.

This work was performed under the JET Contract No. JT9/14673.

References

[1] Abe, H., Momota, H., Itatani, R. and Fukuyama, A., Phys. Fluids **23** (1980) 2417.

[2] Alava, M.J. and Heikkinen J.A., Plasma Phys. Contr. Fusion **34** (1992) 957.

[3] Alava, M.J. and Heikkinen J.A., Phys. Fluids **B4** (1992) 13.

[4] Berro, E.A. and Morales, G.J., IEEE Trans. Plasma Sci. **18** (1990) 142.

[5] Brambilla, M., Nucl. Fusion **28** (1988) 549.

[6] Brambilla, M., Chodura R., Hoffmann J. et al., in: Plasma Physics and Controlled Nuclear Fusion Research 1990, IAEA 1991, Vol. 1, 723.

[7] Bureś, M., Avinash, K., Brinkschulte, H. et al., Bull. Am. Phys. Soc. **33** (1988) 2032.

[8] Bureś, M., Brinkschulte, H, Jacquinot, J., Lawson, K.D, Kaye A. and Tagle, J.A., Plasma Phys. Contr. Fusion **30** (1988) 149.

[9] Bureś, M., Jacquinot, J., Start, D.F.H. and Brambilla, M., Nucl. Fusion **30** (1990) 251.

[10] Cardinali, A. and Romanelli F., Phys. Fluids **B4** (1992) 504.

[11] Chiu, S.C, Chan, V.S., Perkins, F.W and Puri, S., Phys. Fluids **B3** (1991) 159.

[12] D'Ippolito, D.A., Myra, J.R., Bureś, M. and Jacquinot, J. Plasma Phys. Contr. Fusion **33** (1991) 607.

[13] Evrard, M.P. and Weynants, R.R., Proc. 3rd Varenna–Grenoble Int. Symp. on Heating in Toroidal Plasmas, Grenoble 1982, Vol 1, 339.

[14] Faulconer, D.W., 11th Eur. Conf. on Controlled Fusion and Plasma Physics, Aachen 1983, EPS, Vol. 7D, Part II, 123.

[15] Fukuyama, A., Itoh, K. and Itoh, S., Comp. Phys. Rep. **4** (1986) 137.

[16] Gradov, O.M. and Stenflo, L., Plasma Phys. **22** (1980) 727.

[17] Harms, K.D., Hasselberg, G. and Rogister, A., Nucl. Fusion **14** (1974) 657.

[18] Heikkinen, J.A., Phys. Lett. **152A** (1991) 205.

[19] Heikkinen, J.A. and Avinash, K., Nucl. Fusion **29** (1989) 1307.

[20] Heikkinen, J.A. and Bureś, M., Plasma Phys. Contr. Fusion **32** (1990) 173.

[21] Jaeger, E.F., Batchelor, D.B., Carter, M.D. and Weitzner, H., Nucl. Fusion **30** (1990) 505.

[22] Karney, C.F.F. and Bers, A., Phys. Rev. Lett. **39** (1977) 550.

[23] Majeski, R., Tanaka, T., Intrator, T., Hershkowitz, K., Ko, K., Grossmann, W. and Drobot, A., Fus. Engrg. Design **12** (1990) 31.

[24] Noterdaeme, J.-M. et al., Fus. Engrg. Design **12** (1990) 127.

[25] Ono, M., Wong, K. and Wurden, G.A., Phys. Fluids **26** (1983) 298.

[26] Skiff, F., Ono, M., Colestock, P. and Wong, K.L., Phys. Fluids **28** (1985) 2453.

[27] Stix, T., *The Theory of Plasma Waves,* (Mc Graw-Hill, 1962).

[28] Tagle, J.A., Laux, M., Clement, S. et al., Fus. Engrg. Design **12** (1990) 217.

[29] Van Nieuwenhove, R., Durodié, F., Koch, R., Van Oost, G. and Matsumoto, K., Fus. Engrg. Design **12** (1990) 203.

[30] Van Nieuwenhove, R., Van Oost, G., Beuken, J.M. et al., in Contr. Fusion and Plasma Heating, (Proc. 15th Eur. Conf., Dubrovnik 1988), Vol.12 B, Part II, EPS (1988) 778.

[31] Van Nieuwenhove, R., Van Oost, G., Noterdaeme, J.M., Brambilla M., Gernhardt, J. and Porkolab, M., Nucl. Fusion **28** (1988) 1603.

[32] Wesner F., Prozesky, V.M., Behrisch R. and Staudenmaier, G., Fus. Engrg. Design **12** (1990) 193.